

# International Conference on Space Optics—ICSO 2008

Toulouse, France

14–17 October 2008

*Edited by Josiane Costeraste, Errico Armandillo, and Nikos Karafolas*



## *Optical communications between an aircraft and a geo relay satellite: design and flight results of the LOLA demonstrator*

*L. Vaillon*

*G. Planche*

*V. Chorvalli*

*L. Le Hors*



## OPTICAL COMMUNICATIONS BETWEEN AN AIRCRAFT AND A GEO RELAY SATELLITE: DESIGN & FLIGHT RESULTS OF THE LOLA DEMONSTRATOR

L. Vaillon<sup>(1)</sup>, G. Planche<sup>(2)</sup>, V. Chorvalli<sup>(3)</sup>, L. Le Hors<sup>(4)</sup>

*EADS Astrium Satellites, 31 rue des cosmonautes, 31077 Toulouse France*

<sup>(1)</sup>[ludovic.vaillon@astrium.eads.net](mailto:ludovic.vaillon@astrium.eads.net), <sup>(2)</sup>[gilles.planche@astrium.eads.net](mailto:gilles.planche@astrium.eads.net),  
<sup>(3)</sup>[vincent.chorvalli@astrium.eads.net](mailto:vincent.chorvalli@astrium.eads.net), <sup>(4)</sup>[lennaic.lehors@astrium.eads.net](mailto:lennaic.lehors@astrium.eads.net),

### ABSTRACT

On December 5<sup>th</sup>, 2006, a laser link was for the first time established between an optical terminal on-board an aircraft flying at 9,000 m and the SILEX terminal on the Artemis geostationary satellite. This world first event was the result of the 3-year demonstration program LOLA performed by EADS Astrium for the arms procurement agency of the French Ministry of Defense (DGA) to investigate the feasibility of high data rate optical communications through the atmosphere. This first link was followed by a 6-month flight test campaign totalizing more than 50 successful communication sessions over 20 flights. The campaign allowed assessing the operational link performances (bit error rate before and after decoding, availability) in a variety of flight conditions (altitude & weather) and to correlate the model of optical propagation in the atmosphere. The test campaign was concluded by real-time data transmission offering HD video quality between the aircraft and the DGA stand at the Paris "Le Bourget" Air Show.

In addition to the technical challenges common to instruments with sub- $\mu$ rad pointing requirements (e.g. highly stable structures), optical communications set specific challenges on the optical design and on the detection chain.

- High level of isolation between emission & reception to handle the huge ratio ( $\sim 10^9$ ) between emitted & received laser power levels ( $\sim 150$  mW and 20 to 200 pW);
- Efficient straylight protection to communicate with the Sun down to 5 deg from the field of view;
- Accurate co-alignment between emission & reception directions

### 1 INTRODUCTION

In Europe, the in-orbit success of the SILEX (Satellite Interlink EXperiment) program has demonstrated the feasibility to establish long distance optical links between a LEO remote sensing satellite, namely SPOT4 and the GEO data relay spacecraft ARTEMIS (see for instance [1]). Urgent images taken far away from Europe can be disseminated in near real time to different processing centers over the large geographical area covered by the GEO relay. In the context of a competition with the USA and also Japan where ambitious programs are on-going, Europe has continued to invest in optical communication technologies. The European Space Agency has promoted several Optical Intersatellite Link technology developments and is currently defining the future European Data Relay Satellite (EDRS) to take over the Artemis GEO relay around 2012 and offer high data rate optical links with demanding users like GMES Sentinel LEO missions. The German Space Agency (DLR) is funding the LCT (Laser Communication Terminal) program currently flown on board the TerraSAR satellite to demonstrate LEO-LEO optical communications. In France, the LOLA program successfully conducted in 2004-2007 by EADS Astrium for the French MOD has confirmed the European leadership in optical communications, with the world first link through the atmosphere between a GEO satellites and an aircraft.

After a brief overview of the LOLA program (more details can be found in [2]), this paper is focused on the innovations introduced in the optical system to face the challenges of an airborne terminal and laser propagation in the atmosphere. Finally, a synthesis of the performances measured during the flight test campaign is presented, which demonstrated the feasibility & robustness of optical data transmission in the atmosphere.

## 2 OVERVIEW OF THE LOLA PROGRAMME

LOLA stands for Liaison Optique Laser Aéroportée (Airborne Atmospheric Laser Link). The main objective of this prospective program was to characterize the performance of an optical link between a demonstrator of an airborne optical terminal and the SILEX terminal flying on-board the ARTEMIS geostationary spacecraft (cf. fig.1.). Optical links from the ground have also been successfully performed. A demonstrator of a future airborne optical terminal has been developed (see next section) and flown during the 6-month test campaign on a Falcon 20 from the CEV (Centre d'Essais en Vol), the French aeronautical test centre. Despite the numerous functional & technology innovations introduced to simplify the terminal design, the overall development took less than 2.5 years, from go-ahead early 2004 to terminal integrated in the aircraft in October 2006.

The data link characteristics are imposed by the SILEX system, both in terms of data rate (2 Mbit/s uplink and 50 Mbits/s downlink), laser wavelength (0.8  $\mu\text{m}$ ) and OOK (On-Off Keying) modulation. Higher data rates, up to 360 Mbit/s per channel, are however possible with the same flight-proven 0.8  $\mu\text{m}$  laser technology. In order to ensure the quasi error-free (bit error rate  $< 10^{-9}$ ) data transmission despite large & fast signal fading introduced by laser propagation in the atmosphere, specific coding of the data stream is implemented.



Fig. 1: The LOLA bi-directional optical data link between an aircraft and the Artemis GEO Relay satellite

## 3 LOLA OPTICAL TERMINAL DESIGN & PERFORMANCES

### 3.1 Opto-mechanical architecture

The LOLA optical terminal (Cf. Fig. 2 & Fig. 3) features an aerial opto-mechanical assembly conceived as a technology demonstrator for future airborne &

space terminal, and PC-based communication and control electronics housed in standard racks (not shown on the figures). The terminal is placed in front of an aircraft window, modified to avoid wave front distortion of the laser beams. The aerial includes a telescope mounted on top of an hemispherical pointing mechanism and the collected & emitted laser signals are transmitted through a coudé optical arrangement to the focal plane located on the fixed part (cf. Fig. 4).

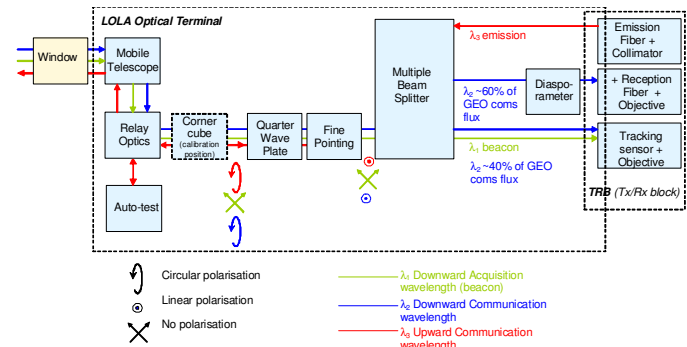


Fig. 2: Optical architecture

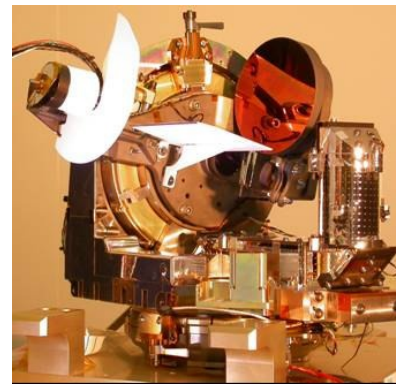


Fig. 3: LOLA terminal aerial during ground tests in clean room



Fig. 4: SiC focal plane prior to integration

### 3.2 Telescope assembly

The telescope is a TMA (Three Mirror Anastigmat) afocal telescope with 125 mm circular aperture. The optical combination is an off-axis Korsch telescope without central occultation aperture (see Fig. 5), composed of three aspherical mirrors realizing an optical magnification of 20. A fourth flat mirror is used

to fold the optical beam in order to minimize the telescope volume. The output beam is perpendicular to the line of sight to allow telescope rotation about its elevation axis. The whole telescope is realized in Silicon Carbide (SiC), the high performance material mastered by Astrium for building stable structures for space optical instruments.

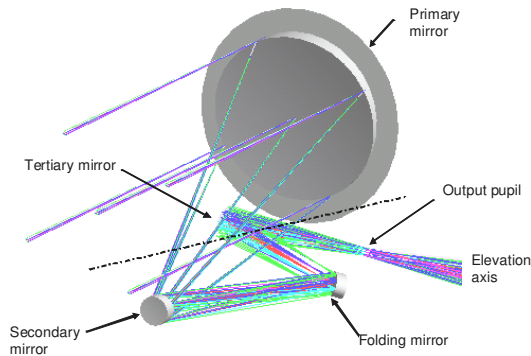


Fig. 5: Telescope optical layout

The measured optical performances are excellent, with a wave front error (WFE) of 15 nm rms (excluding focus), i.e.  $\lambda/55$  rms and a total transmission of 97%. The optical quality is mainly affected by the M1/M2 relative stability, which is kept below 5  $\mu\text{m}$  (resp. 10  $\mu\text{m}$ ) in the transverse (resp. longitudinal) direction.

Background signal due to straylight from the Sun being a performance driver for the tracking sensor, efficient baffling is required. The baffle design was optimized and verified by detailed analysis using the ASAP software tool. The folding mirror (FM), used at high incidence ( $\sim 48$  deg) shall in particular be efficiently protected since it would create large Sun diffusion close to the optical axis. This is the role of the baffles around M2 and between M1-M2 and M2-FM beams (see Fig. 6 and Fig. 3).

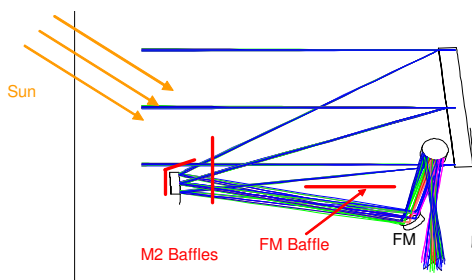


Fig. 6: Telescope baffle design

The straylight immunity was thoroughly verified by tests with a Sun simulator, first at aerial level and after completion of terminal integration, including also the window. After some minor modifications of the baffles, full straylight immunity was demonstrated for the terminal sighting down to 5 deg from the Sun direction. The window was found to have no straylight impact as

long as reflections on the mounting edge are prevented by adequate absorbing coating.

### 3.3 Coudé transmission to the focal plane

The optical relay assembly (ORA) is in charge of transporting the signal collected by the mobile telescope (exit of elevation axis) towards the focal plane located on the fixed part:

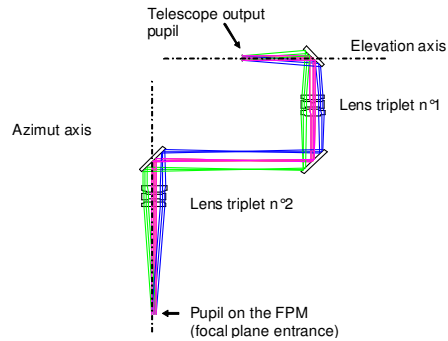


Fig. 7: ORA optical layout

The ORA is composed of three flat mirrors and two lens triplets in charge of conjugating the telescope output pupil at the entrance of the focal plane. The optical beams follow the hollow axes of the wide angle pointing mechanism. The measured ORA performances are a WFE (excluding focus) of 17 nm rms ( $\sim \lambda/50$ ) and transmission of 95% @800 nm and 99% @850 nm.

### 3.4 Focal plane

The focal plane, also build in SiC, is carrying all the active & passive elements in charge of acquisition & tracking, communication laser emission & reception and laser beams routing.

The acquisition & tracking function is composed of the fine pointing mechanism (FPM) and of the acquisition/tracking sensor (ATS), further detailed in section 3.5. The FPM is a 2-axis fast steering mirror manufactured by Oerlikon Space AG, with a small angular range ( $\pm 5$  mrad), high resolution (1  $\mu\text{rad}$  peak-to-peak noise) and large bandwidth (1.5 kHz). Such high performances, with the capability to reject dynamic disturbances up to 700 Hz, are required to accurately track the received signal and reach the 2.5  $\mu\text{rad}$  ( $2\sigma$ ) pointing accuracy in the harsh vibration environment of an aircraft.

The laser Rx and Tx communication electronics, embedding laser diodes and avalanche photodiodes, are connected via optical fibers to the focal plane, allowing to remove from the terminal stable core these large and dissipating devices. The focal plane only implements the receive & transmit fibred collimators and the beam splitter to separate the received beam between tracking

& communication channels (see Fig. 2). A high pointing stability between all channels shall be ensured, with as main challenge a tight co-alignment ( $0.5 \mu\text{rad}$ ) between the emission direction and the tracking reference provided by the tracking sensor (ATS). This is obtained by mounting the receive objectives & the emission collimator on a common SiC structure (see Fig. 8), but also thanks to their specific design developed by EADS Sodern for demanding applications like star tracker and PHARAO. This allows very low sensitivity to temperature within the  $20^\circ \pm 5^\circ\text{C}$  operational environment. Moreover, the stability of the co-alignment is measured prior to each communication session by retro-reflecting the emitted signal on the ATS thanks to a corner cube placed in the optical path by a flip-flop mechanism and can be compensated by biasing the tracking reference on the ATS. The narrow interferential filters used to block the broadband background signal are implemented in front of each objective.

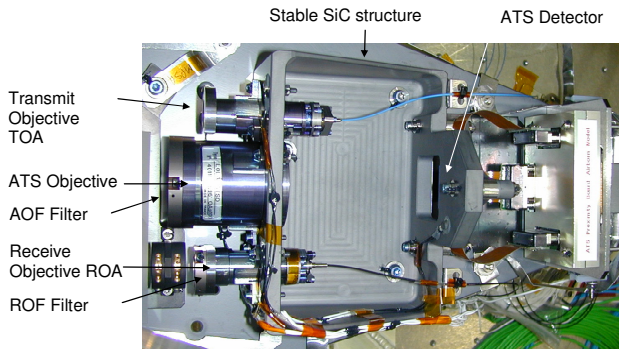


Fig. 8: Emit/receive assembly

With the objective of reducing focal plane mass & volume, all the functions required for filtering and routing the three wavelengths (beacon 800 nm, received coms 820 nm and emitted coms 850 nm) were integrated in a single device, the MPS (Multiple Path Splitter, patented design). The MPS (see Fig. 9) is composed of glass prisms bonded on a plate made of Invar for good thermo-elastic compatibility with the SiC focal plane. The use of optical invariants ensures that the MPS motions do not degrade the emission/reception co-alignment. The filtering of emission and the diplexing of emission/reception is ensured by a set of 3 prisms with a dichroic coating at the inner interface. The measured transmission (see Fig. 10) shows little sensitivity to the field angle thanks to small incidence angle.

In order to allow flexibility in operations and characterization, the apportionment of the received signal between the tracking sensor (ATS) and the communication receiver is performed by another set of two prisms with a polarization-sensitive coating: the non-polarized beacon is fully transmitted towards the

ATS, while the linearly -polarized communication signal is distributed according to the ratio of the in-plane & out-of-plane components. The tunable half wave plate allows manual adjustment of the polarization direction, and thus the apportionment between tracking & communication channels

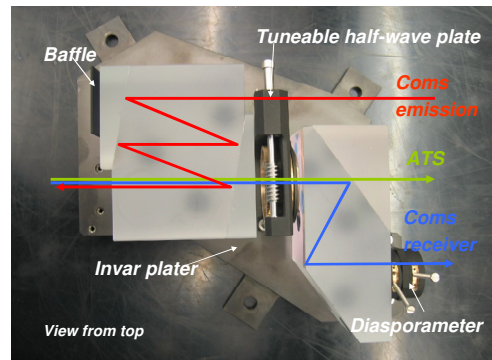


Fig. 9: MPS top view with laser signals paths

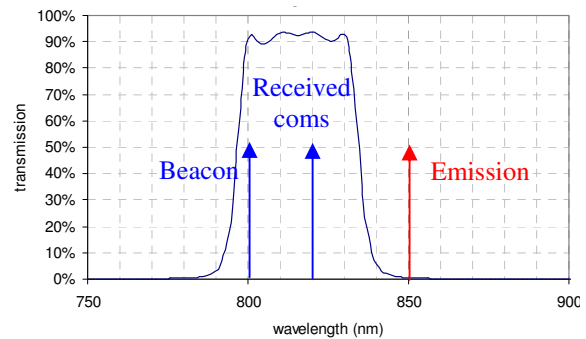


Fig. 10: Dichroic coating transmission for emission & reception diplexing

### 3.5 Acquisition & tracking sensor (ATS)

Thanks to the windowing capability offered by the CMOS technology, the distinct acquisition & tracking CCD sensors of SILEX are combined in a single Acquisition and Tracking Sensor (ATS). This sensor (see Fig. 11) is part of the suite of CMOS imaging array detectors developed by Astrium in cooperation with ISAE/CIMI (France), like the COBRA2M 2Mpixel array to be flown on the GOCI instrument of the Korean COMS satellite. In acquisition mode, the whole  $750 \times 750$  pixel array is read at a rate of 10 Hz (16 Mpix/s), while in tracking mode, a small window centered on the tracking reference is read at 12 kHz. A bias is applied on the tracking reference of the ATS to compensate for the so-called “point-ahead angle” ( $20 \mu\text{rad}$  offset between receive an emit direction due to limited light velocity), thus removing the need for a dedicated mechanism (Point Ahead Assembly in SILEX) with sub- $\mu\text{rad}$  accuracy.

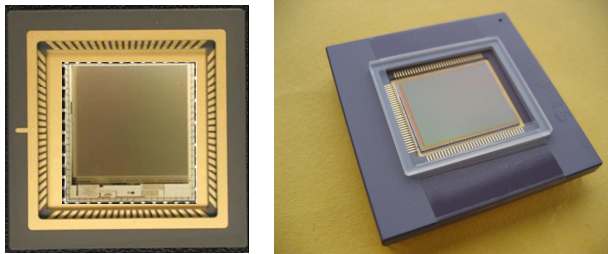


Fig. 11: CMOS detectors: Left: LOLA ATS (750x750 pixel), right GOCI/COMS Cobra2M (2 Mpixels)

### 3.6 Optical window

The aircraft window used for terminal sighting is replaced by a high optical quality 40 mm silica plate with slightly wedged faces to avoid interferences. The outer face of the window is coated with a high resistance anti-reflection coating to resist external aggression due to rain, dust or ice. The inner face implements a high pass filtering coating removing about 50% of the solar flux, to avoid terminal heating when the Sun enters the cavity.

Despite its high optical quality, the window is a major contributor to terminal performance because it withstands high mechanical loads due to inner/outer pressure difference (250 mbar at the 9,000 m max flown altitude) and large thermal gradients due to temperature mismatch between terminal cavity (~20°C) and outside air (~-40°C). Moreover, an air drying system is required to prevent freezing on the cold window.



Fig. 12: The optical window mounted on an emergency door of the aircraft

## 4 FLIGHT TEST CAMPAIGN

### 4.1 Overview

After a comprehensive ground validation campaign, the terminal was integrated in an enclosure providing a suitably clean & dry environment (in particular to prevent water condensation and icing on the cold window). The package was then moved to the CEV

flight test facility in Istres in the south of France and mounted in a Falcon 20 aircraft.

The terminal enclosure is thermally controlled using an air conditioner, but due to the large coupling with the cabin and the cold window, and the need to switch off during communication sessions to avoid turbulences, the terminal experienced large temperature variations during the flights (up to 10 °C). Hopefully, the low sensitivity of the opto-mechanical design to thermal variations and gradients was verified, and the pointing accuracy remained within the expected range. The control & communication electronics are integrated in standard aeronautical racks, and the terminal is operated by a flight engineer from the control console.

Sighting through a window is imposed by the constraint of avoiding aircraft external shape modification requiring flight re-qualification. In an operational application, the terminal would be hosted in a turret allowing hemispherical pointing. For the demonstration, the direction of flight was therefore imposed (roughly ENE) to sight Artemis on its 10°N geostationary slot (see Fig. 13). Air traffic regulations in-turn limit the straight line flight duration to about 20 min, thus limiting the duration of the communication session. Accounting for the constraint of returning to the initial rendezvous point, only three 20-min sessions can be performed during a 3-hour flight.

The rendezvous with Artemis is programmed by ESA's operators at least 24h in advance, once meteorology & air traffic regulation constraints have been cleared. Then the flight is scheduled to have the aircraft flying at the rendezvous point with a 10 km / 2 sec accuracy.

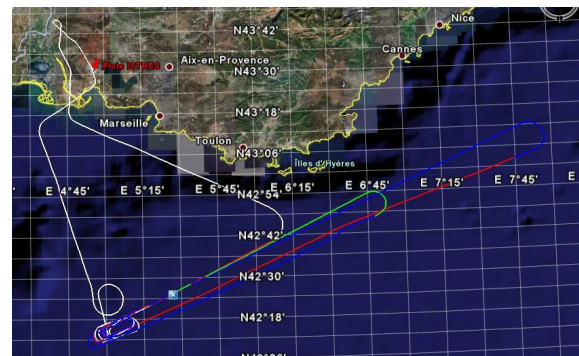


Fig. 13: Typical flight path with the rendezvous point at the bottom left

The test campaign started in November 2006 by a 1-month phase dedicated to the validation of the terminal functional behaviour and verification of the pointing performances, realised through acquisition tests from the ground and three flight tests. No data exchange was performed through the optical link because the communication electronics, not available yet, were replaced by a continuous-wave laser source and a power meter receiver. This phase was successfully concluded

on December 5th, 2006, with the world first laser link between the aircraft flying at 9,000 m and the Artemis geostationary satellite. For each of the three rendezvous, the acquisition was performed in less than 10 sec (from the start of the beacon scan to the link locking) and the tracking was maintained during 10 min until the link was interrupted by aircraft 180° turn

Communication electronics were integrated early 2007 and a 5-month flight test period started, aiming at characterising the link performances sensitivity to flight conditions (e.g. altitude & weather conditions). The test campaign was concluded by five flight demonstrations, a first one end of May in Toulouse for the French MoD representatives and five lasts during the Paris Airshow at Le Bourget, totalising ten 15-min. sessions of real-time video data transmission from the airplane flying in the south of France.

#### 4.2 Acquisition performances

A key issue in optical communication is the capability to point each terminal towards the other before the incoming laser signal is detected (so-called “a priori pointing”). The pointing reference of the LOLA terminal is computed from the ephemerides of the Artemis satellite and the attitude & position measurements with an IXSEA/PHINS inertial measurement unit (IMU). The bias between the IMU and the telescope line of sight, accurately characterised on ground during terminal integration, is compensated for in the pointing reference.

Fig. 14 shows the position in the terminal FoV (Field of View) of the first beacon spot detection for more than 50 acquisitions. The position of the detected spot measures the a priori open-loop steering error (up to 2 mrad), showing the good sizing of the +/-2.5 mrad FoV.

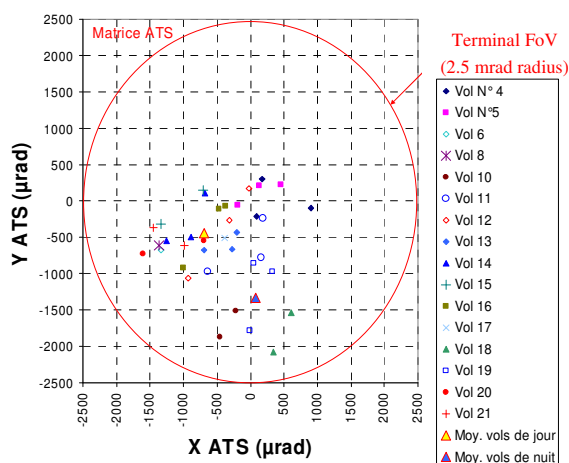


Fig. 14: A priori pointing error measured over more than 50 link acquisitions

The error is not evenly distributed in the FoV, with a concentration in the -X/-Y quadrant, showing a systematic component that could be corrected.

Moreover, the error decreases between the first and the last sessions of a flight in azimuth direction, showing a probable effect of the IMU drift. Finally, thermal effects are significant because of the impossibility to accurately regulate the terminal temperature, as pointed out in the previous section. Fig. 14 illustrates the thermal sensitivity, with an average pointing error different for day (X = -0.7 mrad, Y = -0.45 mrad) and night (X = 0.1 mrad, Y = -1.3mrad) flights, where the terminal temperature is significantly lower. These effects justify of the attention paid to minimise terminal thermo-elastic deformation, e.g. by selecting Silicon Carbide (SiC) high performance material for telescope & focal plane opto-mechanical parts.

#### 4.3 Tracking performances

After a convergence process, the tracking of the beacon signal is initialised. The average received beacon signal is weak, 10 to 30 pW, depending on the attenuation due to cirrus clouds. The communication phase starts when the communication signal is received from the GEO terminal after a similar convergence phase. The average received signal is higher (generally ~180 pW but down to 60 pW in some difficult sessions with a cirrus cover). Nevertheless, with an integration time reduced from 500 µsec for beacon to 85 µsec (12 kHz sampling) to allow higher tracking bandwidth, the signal-to-noise ratio on the detector is often similar.

The signal is highly variable due to scintillation caused by propagation in the atmosphere, with standard deviation increasing at low altitude, around 10% at FL300 (9,000 m) and 20% at FL210 (6,000 m), but also largely depending on the turbulence level (the worst case RMS value of 33% was measured at 9,000 m).

Any pointing error (due to terminal or tilt during propagation on the atmosphere) induces a loss in the signal intensity emitted towards the other terminal. These losses are contributors in the link budget, which allocates at most 3 dB to this parameter. The terminal pointing error is not directly measurable in flight since the resulting attenuation of the signal received by the GEO relay cannot be separated from atmospheric propagation effects (attenuation & scintillation).

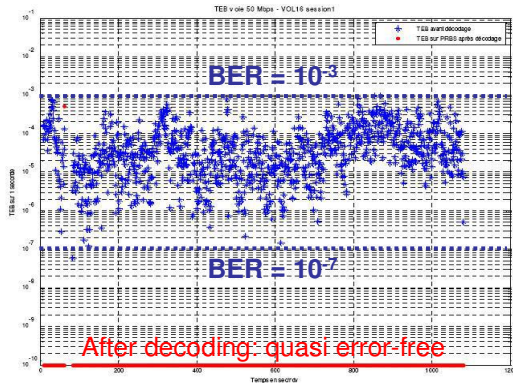
The terminal pointing error is specified as the bias term plus 2-sigma dynamic variation, 3.5 µrad for beacon tracking and 2.5 µrad for communication tracking. In flight, the dynamic tracking error is measured on the ATS (difference between measured spot centre and tracking reference, with zero mean due to closed-loop control). This tracking error also includes the residual atmospheric tilt of the received signal not compensated by the tracking loop, so the flight measurements are compared to the dynamic allocation of the above requirement augmented by the allocation to uncorrected atmospheric tilt. The following table shows that the measured performance is excellent, about a factor of

two better than required, mainly because the tracking bandwidth (300 to 700 Hz depending on sessions) was eventually larger than assumed in the analyses that supported budget allocation. The tracking performance is better in communication (because of the increased bandwidth) and at higher altitude because the atmospheric tilt is reduced

| Tracking error (μrad) |             | Beacon tracking |      | Coms tracking |      |
|-----------------------|-------------|-----------------|------|---------------|------|
|                       |             | X               | Y    | X             | Y    |
| FL300                 | In-flight   | 0.85            | 0.93 | 0.67          | 0.69 |
|                       | Requirement | 1.73            | 1.73 | 1.55          | 1.55 |
| FL210                 | In-flight   | 0.65            | 0.72 | 0.53          | 0.55 |
|                       | Requirement | 1.45            | 1.45 | 1.24          | 1.24 |

#### 4.4 Communication performance

The communication performance is measured in both directions by computing the bit error rate (BER), the ratio of the number of false bits to the total number of bits in the same duration. The BER is computed on the raw data and after decoding the data with the error correction code introduced at emission to handle dynamic fading of the signal due to scintillation. The following discussion is focused on the uplink (user to relay) which features the largest bit rate (50 Mbit/s). Fig. 15 shows BER computed during an average session (in terms of atmospheric propagation) during a flight at 6,000 m.



The anomaly around  $t = 60$  sec corresponds to a change in coding depth and is a transient artefact due to communication software re-initialisation

Fig. 15: BER before and after decoding computed over 2 sec & measured over a 17 min. session

The BER before decoding is highly instationary (between  $10^{-7}$  and  $10^{-3}$ ) depending on the dynamic fading introduced by the atmosphere. It tends to increase at the end of the session when the aircraft is flying over the Alps, where the atmosphere is more turbulent. The error correction code is very efficient, since after decoding the data is error free ( $BER < 10^{-10}$ , i.e. less than one error every 200 sec. Extensive post-processing of the flight data allowed assessing the effectiveness of the error correction code as a function

of the BER before decoding. With  $BER < 10^{-4}$ , the decoded data is error free, while with  $BER > 10^{-2}$ , coding does not bring improvements. Between these values, the effectiveness depends on the coding ratio.

The measurement of the power on the communication receiver also allowed correlating the propagation models supporting the computation of the link budgets. The correlation is excellent on the downlink budget, with a difference between prediction & measurements lower than 5%. It is still very good on the uplink budget (error < 20%) despite the much more complex propagation model due to the proximity of the emission and of the disturbed atmospheric layers.

#### 5 CONCLUSION & PERSPECTIVES

The LOLA program was the opportunity to demonstrate that high data rate optical communications between satellites and airborne or ground users are not only feasible with attractive performance, but also that the overall system can be made robust to signal fading due to propagation in the atmosphere, guarantying a good system availability. The flight test campaign also allowed detailed correlation of the atmospheric propagation model (presented in [2]). The validated model was then used to assess the worldwide availability of aircraft-to-GEO optical links as a function of season and altitude of flight.

Built in continuity with the SILEX precursor program, LOLA was also the opportunity to introduce and test some major technology & functional innovations: SiC material and associated integration techniques to realize stable telescope & focal plane assemblies; fast & accurate wide angle pointing mechanism able to perform signal acquisition; CMOS detector which flexible windowing capability allows to combine acquisition & tracking detection and point ahead angle compensation in a single device. Demonstrating these technologies paves the way for future airborne optical terminals, even though integration into existing airborne turrets allowing hemispherical pointing needs to be further investigated. Such technology assessment also prepares the next generation space optical terminals, to provide an operational data relay function needed for high data rate users, e.g. like the Sentinel missions of the on-going GMES program.

#### 6 REFERENCES

1. "SILEX in-orbit performances", G. Planche, V. Chorvalli, Proceedings of the 5<sup>th</sup> International Conference on Space Optics (ICSO), Toulouse 2004
2. "LOLA: a 40.000 km optical link between an aircraft and a geostationary satellite", V. Cazaubiel, G. Planche, V. Chorvalli, L. Le Hors, B. Roy, E. Giraud, L. Vaillon, F. Carré, E. Decourbey, Proceedings of the 6<sup>th</sup> International Conference on Space Optics (ICSO), ESTEC, 2006